Development 136, 865-875 (2009) doi:10.1242/dev.027565

TNFα-dependent hepatic steatosis and liver degeneration caused by mutation of zebrafish *s-adenosylhomocysteine hydrolase*

Randolph P. Matthews[1], Kristin Lorent[2], Rafael Mañoral-Mobias[2], Yuehua Huang[3], Weilong Gong[2], Ian V. J. Murray[3], Ian A. Blair[3] and Michael Pack[2,4,*]

Hepatic steatosis and liver degeneration are prominent features of the zebrafish *ducttrip* (*dtp*) mutant phenotype. Positional cloning identified a causative mutation in the gene encoding S-adenosylhomocysteine hydrolase (Ahcy). Reduced Ahcy activity in *dtp* mutants led to elevated levels of S-adenosylhomocysteine (SAH) and, to a lesser degree, of its metabolic precursor S-adenosylmethionine (SAM). Elevated SAH in *dtp* larvae was associated with mitochondrial defects and increased expression of *tnfa* and *pparg*, an ortholog of the mammalian lipogenic gene. Antisense knockdown of *tnfa* rescued hepatic steatosis and liver degeneration in *dtp* larvae, whereas the overexpression of *tnfa* and the hepatic phenotype were unchanged in *dtp* larvae reared under germ-free conditions. These data identify an essential role for *tnfa* in the mutant phenotype and suggest a direct link between SAH-induced methylation defects and *TNF* expression in human liver disorders associated with elevated TNFα. Although heterozygous *dtp* larvae had no discernible phenotype, hepatic steatosis was present in heterozygous adult *dtp* fish and in wild-type adult fish treated with an Ahcy inhibitor. These data argue that *AHCY* polymorphisms and AHCY inhibitors, which have shown promise in treating autoimmunity and other disorders, may be a risk factor for steatosis, particularly in patients with diabetes, obesity and liver disorders such as hepatitis C infection. Supporting this idea, hepatic injury and steatosis have been noted in patients with recently discovered *AHCY* mutations.

KEY WORDS: Lipid metabolism, Liver disease, Methionine metabolism, Methylation, TNF alpha, Zebrafish

INTRODUCTION

Hepatic steatosis, the accumulation of lipid within hepatocytes, is a critical step in the pathogenesis of human diseases such as alcoholic liver disease, non-alcoholic fatty liver disease associated with the metabolic syndrome, chronic hepatitis C infection and other disorders. In more severe forms of these conditions, the liver becomes inflamed and fatty liver progresses to non-alcoholic steatohepatitis (NASH). Understanding the factors affecting this progression is vital because steatohepatitis is a risk factor for cirrhosis, liver failure and hepatocellular carcinoma.

Several pathogenic mechanisms appear to contribute to the development of hepatic steatosis and steatohepatitis, and it has been proposed that multiple 'hits' are required for disease progression. Hepatocytes accumulate lipid when its synthesis, uptake, secretion and/or utilization are altered (Browning and Horton, 2004; Fromenty et al., 2004). Although the events that initiate most steatotic disorders are now beginning to be more clearly defined, it has been recognized for many years that methionine metabolism, which is altered in patients with alcoholic liver disease and other chronic liver disorders associated with steatosis, may play a contributory role (Diehl, 2005; Duong et al., 2006; Esfandiari et al., 2005; Innis and Hasman, 2006; Kharbanda, 2007; Lu et al., 2002; Mato et al., 2008; Wortham et al., 2008; Zhu et al., 2003). Mitochondrial dysfunction, endoplasmic reticulum stress, sensitization to cytokine-induced liver injury and reduced methyltransferase activities have all been implicated in mediating the effects of methionine metabolism defects in the mammalian liver.

The recessive lethal zebrafish mutant *ducttrip* (*dtp*) was recovered in a screen for exocrine pancreas mutants (Yee et al., 2005). Initial phenotypic analysis showed normal differentiation of early *dtp* exocrine progenitors, whereas their proliferation, terminal differentiation and survival were disrupted at later stages (Yee et al., 2005). Subsequent experiments, described in this report, reveal hepatic steatosis, mitochondrial dysfunction and liver degeneration in all *dtp* larvae, as well as a milder phenotype in adult heterozygous *dtp* carriers. Positional cloning identified a causative mutation in the gene encoding S-adenosylhomocysteine hydrolase (Ahcy), the enzyme that hydrolyzes S-adenosylhomocysteine (SAH) to homocysteine and adenosine, a pathway that has been linked to mitochondrial dysfunction (Song et al., 2007) and hepatic steatosis. These findings argue that a heritable reduction in Ahcy activity may be a predisposing genetic risk factor for hepatic steatosis. Consistent with such a role for AHCY in humans, steatosis and liver injury were reported in hypermethioninemic patients recently shown to carry homozygous *AHCY* mutations (Baric et al., 2005; Baric et al., 2004; Buist et al., 2006).

MATERIALS AND METHODS

Fish lines

Procedures for mutagenesis and screening for *dtp* are reported elsewhere (Yee et al., 2005). Heterozygous adult males were used for all studies of *dtp* carriers; fish were identified by genotyping (details available upon request). Wild-type TLF strain fish were used for all morpholino injections and drug treatments.

[1]Division of Gastroenterology, Hepatology, and Nutrition, The Children's Hospital of Philadelphia and Department of Pediatrics, [2]Department of Medicine, [3]Centers for Cancer Pharmacology and Excellence in Environmental Toxicology and [4]Department of Cell and Developmental Biology, University of Pennsylvania School of Medicine, Philadelphia, PA 19104, USA.

*Author for correspondence (e-mail: mpack@mail.med.upenn.edu)

Accepted 31 December 2008

Genetic mapping and positional cloning of the *dtp* locus

To generate larvae for mapping, *dtp* carriers were mated with wild-type WIK zebrafish, and their progeny were subsequently mated to screen for mutant *dtp* hybrids. Standard Z-markers were used to perform coarse mapping of *dtp* to chromosome 6. Available in silico sequences were used to derive closer dinucleotide repeat markers. Primer sequences for *ahcy*, *chmp4b* and *eif2s2* were obtained from in silico sequences (www.sanger.ac.uk) and individual exons were sequenced. The marker within *ahcy* reflects the actual mutation, which takes advantage of the T-to-C mutation that removes an *Nla*III (CATG) site in exon 8. This polymorphism is the zero recombinant polymorphism. For the wild-type mRNA, a full-length EST was obtained (www.openbiosystems.com) and engineered into pCS2(+); mRNA was then synthesized using mMessage mMachine (Ambion). For the mutant mRNA, the mutation was introduced using site-directed mutagenesis and the mRNA was synthesized identically to that of the wild type.

Mass spectroscopy

Whole larvae were snap-frozen in a dry-ice bath prior to mass spectroscopy for SAM, SAH and AHCY. For SAM and SAH, a mixture of internal standards (250 ng/ml each of [^{2}H3]-SAM and [^{13}C5]-SAH) was added to the tube containing larvae. Larvae were resuspended in ascorbic acid, sonicated and protein isolated by methanol precipitation. An aliquot of the supernatant was analyzed by mass spectrometer (TSQ 7000, Thermo Finnigan), with chromatography on a YMC ODS S-3 column (Waters, Milford, MA, USA) on a linear gradient of water and acetonitrile at 4°C. The ratio of peak area for the analyte to its stable isotope internal standard was used to calculate the concentrations of SAM and SAH. Data for each time point and condition represent means of at least three pairs of larvae measured separately, with s.e.m. indicated.

Tissue preparation and staining

Adult male genotyped heterozygotes, drug-treated fish or control were prepared as indicated elsewhere in the text. Livers were removed immediately following sacrifice, fixed in paraformaldehyde, and then processed. Portions of the livers were also saved for RNA isolation or mitochondrial preparation for GSH determination. Larvae and livers were stained using Hematoxylin and Eosin in accordance with standard methodology. Staining with Oil Red O was performed by first washing sections in 60% triethyl phosphate, then staining in 1% Oil Red O in triethyl phosphate, followed by rinsing and counterstaining in Celestin Blue (www.ebsciences.com/histology/gma_oilredo.htm).

Larvae for sectioning were obtained and processed in glycol methacrylate as described (Wallace and Pack, 2003), except that tissue was processed directly in glycol methacrylate following fixation to avoid lipid extraction. RNA was isolated using Trizol (Invitrogen) and RNAeasy (Qiagen) as described previously for larval zebrafish (Matthews et al., 2004).

In situ hybridization and Ahcy immunostaining

In situ hybridizations were performed on staged embryos and larvae as described (Matthews et al., 2004). Genotyped embryos were used for the TNFα rescue experiments. An anti-human AHCY antibody (Abcam) was used for immunohistochemistry following standard procedures.

Adult 3-deaza-adenosine treatment, mitochondrial preparation and GSH determination

Adult TLF siblings were treated with 2.5 mg/ml 3-deaza-adenosine in system water for the times indicated. Mitochondria were isolated from whole larvae or adult livers using the Mitochondrial Isolation Kit (Sigma). Glutathione concentrations were determined spectrophotometrically using the Glutathione Assay Kit (Sigma).

Morpholino and mRNA injections

Morpholinos (Gene-Tools) were (5′ to 3′): AHCY-5′, CATGTTGACGTTGTGCTGTCTGGTA; AHCY-IE8, CTCAAAGTGTCTTTAAAACACACAC; TNFα-5′, AGCTTCATAATTGCTGTATGTCTTA; TNFα-IE4, TTGATTCAGAGTTGTATCCACTAGG. Morpholinos to *ahcy* and *tnfa* were injected into the yolk at 2 dpf, as described previously (Stenkamp and Frey, 2003). Injection of the *ahcy* AUG morpholino or splice donor (exon 8) morpholino had similar effects. Injection of the *tnfa* AUG morpholino or splice donor (exon 5) morpholino also had similar effects. Knockdown was confirmed using the antibody directed against Ahcy or TNFα described above.

Injections of mRNA (10 pg) were performed at the 1-cell stage, as described previously (Matthews et al., 2005). mRNA of wild-type or mutant *ahcy* was synthesized using standard methods. Injection of azacytidine (azaC) was performed at 2, 3 and 4 dpf by injecting 1 mg/ml azaC (in water) into the yolk in volumes comparable to the morpholino injections.

Western blots and methylcytosine staining

Protein and genomic DNA extractions were performed on midsections of 5-dpf larvae using standard protocols. Western blotting was performed using a standard protocol; antibodies were obtained from Abcam.

For the immuno-slot blot, genomic DNA was denatured and applied to nitrocellulose paper on a slot filtration apparatus (Bio-Rad), and hybridized following the Bio-Rad protocol. Methylcytosine staining was performed using an anti-methylcytosine antibody (GeneTex, Abcam) and the remainder of the protocol was identical to a standard western blotting protocol, except for the use of Tris-buffered saline. Genomic DNA was counterstained with Methylene Blue. Quantification was performed using ImageJ or Adobe Photoshop, which produced identical results.

Quantitative PCR

Real-time quantitative PCR was performed on 4-dpf midsections, as described (Matthews et al., 2004). Primer pairs used for amplification were as published (Lorent et al., 2004; Matthews et al., 2004) or as follows (5′ to 3′): tnfa-F3, GAGCCTGAATCTGAAAATCTGTGG; tnfa-B5, CAGTCTGTCTCCTTCTCGTAAATGG; srebp1-F2, GGAGAACCTGACACTGAAGATGGC; srebp1-B1, TGACTCTACACAGAAACACACACGG; pparg-F1, TGAAAAATGCCCTGCCTGATG; pparg-B1, GGAAAAAACCCTGAGATGTCTGG; gpx-le1, GCTGTTCAGCCTGGACTTTT; gpx-ri1, CGTTGCTGAGTTTGGACTTTT; trx-le1, CTTCGACAACGCCCTAAAAA; trx-ri1, ATTTAAAGTACGGCCCGATG. Data points represent the mean of at least three sets of 4-5 pooled midsections, with s.e.m. indicated. Statistical significance was determined using Student's *t*-test.

RESULTS

Hepatic steatosis in *dtp* mutants

The recessive lethal *dtp* mutation was identified in a chemical mutagenesis screen for zebrafish pancreas mutants (Yee et al., 2005). Homozygous *dtp* larvae, which survive to 9-10 days post-fertilization (dpf), have minimal exocrine tissue but show normal endocrine development (Yee et al., 2005). Subsequent work identified severe liver defects in all homozygous *dtp* larvae beginning at 3 dpf. Histological analyses showed a small, necrotic-appearing liver in 5-dpf mutants, although initial changes in hepatocyte appearance were manifest at 3 dpf (Fig. 1A-J). Ultrastructural examination of 5-dpf *dtp* hepatocytes revealed condensation of mitochondrial cristae, with widening and rarefication of the matrix between the inner mitochondrial membrane and the cristae, and an accumulation of lipid globules (Fig. 1M-P). Oil Red O staining of *dtp* livers confirmed the presence of neutral lipid in the cytoplasm of 5-dpf mutant hepatocytes (Fig. 1K,L). TUNEL and Acridine Orange stainings of 4-dpf and 5-dpf *dtp* larvae were negative (not shown), suggesting non-apoptotic cell death in the mutant liver. These data show that the *dtp* mutation causes progressive liver and exocrine pancreas degradation during the developmental period when cells in both tissues are normally rapidly proliferating. Furthermore, the *dtp* mutation is associated with hepatic steatosis and mitochondrial defects.

Positional cloning of the *dtp* locus identifies mutation of a conserved residue in the *s-adenosylhomocysteine hydrolase* gene

A positional cloning strategy was used to identify the targeted gene responsible for the *dtp* phenotype. High-resolution meiotic mapping of the *dtp* locus defined a 200 kb region on zebrafish chromosome

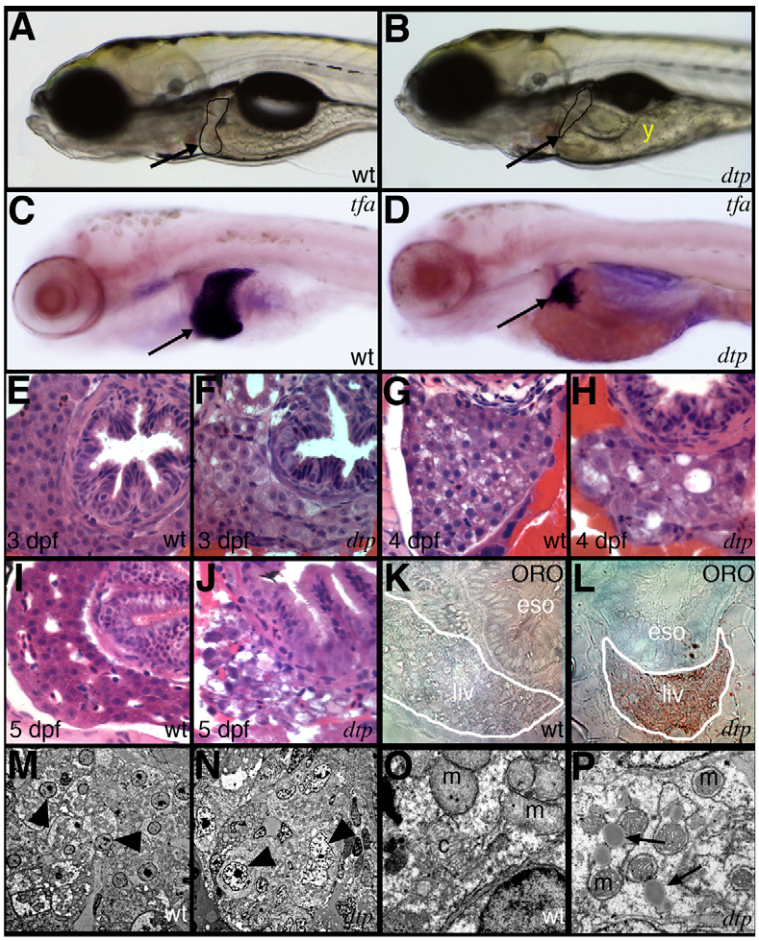

Fig. 1. Hepatic steatosis and liver degeneration in *dtp* zebrafish larvae. (**A-D**) Lateral views of 5-dpf wild-type (wt, A,C) and *dtp* mutant (B,D) larvae showing small liver (outlined, arrow) and reduced yolk consumption (y) in *dtp*. (C,D) RNA in situ hybridization for the liver marker *transferrin* (*tfa*) demonstrates smaller liver size (arrow) in *dtp*. (**E-J**) Liver histology showing irregular *dtp* hepatoctye nuclei beginning at 3 dpf (compare F with E) and with cellular degeneration that is pronounced at 5 dpf (compare J with I). (**K**,**L**) Oil Red O (ORO) staining reveals neutral lipid in the small liver of a 5-dpf *dtp* larva (L) but not in the wild type (K). (**M-P**) Electron micrographs of the enlarged nuclei (compare N with M, arrowheads), mitochondrial defects (compare P with O, m) and lipid droplets (P, arrows) in 5-dpf *dtp* hepatocytes. c, canaliculus; eso,esophagus; liv, liver.

6 that delimited three candidate genes (Fig. 2A), one of which, *ahcy*, was favored because of its established role in methionine metabolism and steatosis. Sequencing of cDNAs derived from *dtp* larvae did not identify mutations in the coding regions of the chromatin-modifying protein 4B (*chmp4b*) or eukaryotic translation initiation factor 2B β2 subunit (*eif2s2*) genes (data not shown). By contrast, a C-to-T transition was present in exon 8 of *ahcy* cDNA recovered from homozygous *dtp* larvae, but not their wild-type siblings (not shown). This missense mutation was predicted to substitute threonine for a methionine residue that is conserved in eukaryotic and prokaryotic Ahcy proteins (Fig. 2B). The methionine residue targeted by the *dtp* mutation resides in the NAD-binding domain (Hu et al., 1999; Hu et al., 2001; Tanaka et al., 2004; Turner et al., 1998), a region of the Ahcy protein that is crucial for enzyme activation (Li et al., 2007). For this reason, we predicted that Ahcy activity was reduced in *dtp* mutants.

Ahcy catalyzes the breakdown of SAH to adenosine and homocysteine and thus plays an important role in methionine metabolism (Fig. 2C). SAH is derived from S-adenosylmethionine (SAM), a methionine metabolite that is considered to be the principal methyl donor used by methyltransferases that modify DNA, RNA, lipids and proteins (Chiang et al., 1996). SAH is a potent inhibitor of methyltransferases (Chiang, 1998; Chiang et al., 1996). Given its important role in methionine metabolism, *ahcy* is predicted to be an essential gene in zebrafish, as suggested by studies in mammals (Miller et al., 1994). As with many zebrafish mutants, survival during early development is most likely explained by maternally supplied *ahcy* mRNA and Ahcy protein, which were both identifiable in zebrafish embryos at 3 hours post-fertilization (hpf) (Fig. 2D,H). Examination of older embryos revealed widespread *ahcy* expression through 24 hpf, but by 48 hpf expression was limited to liver, intestine, pancreas and discrete areas within the brain and eye (Fig. 2B-G). These areas correspond to regions of active cell proliferation, consistent with an essential role of Ahcy in metabolically active cells targeted by the *dtp* mutation. Injection of morpholino antisense oligonucleotides directed against *ahcy* resulted in larval hepatic steatosis, although milder than in *dtp* (see Fig. S1 in the supplementary material) and without significant hepatocyte degeneration (data not shown). Together, tight genetic linkage of *ahcy* to the *dtp* locus, partial *dtp* phenocopy induced by *ahcy* morpholino knockdown, and the established role of methionine metabolism in mammalian hepatic lipid steatosis, strongly support the identification of *ahcy* as the causative gene.

Methionine metabolism is disrupted in *dtp* larvae

Since reduced Ahcy activity is predicted to increase SAH levels and secondarily inhibit a large number of methylation reactions, we hypothesized that the *dtp* liver phenotype might arise from impaired methylation. To explore this hypothesis, we first measured total SAM and SAH levels in *dtp* embryos and larvae and their wild-type siblings using mass spectrometry. In wild-type embryos and larvae, SAH levels were relatively stable between 2 and 5 dpf, while SAM levels increased modestly (Fig. 3A,B, blue lines). By contrast, levels of SAH and SAM were increased in *dtp* mutants during these stages

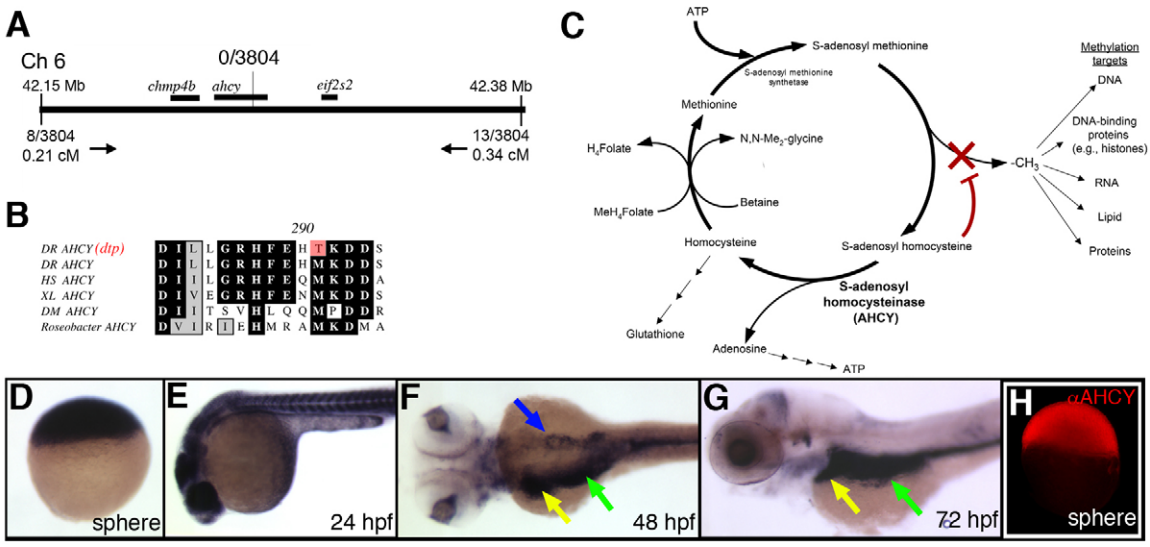

Fig. 2. Identification of *ahcy* as the *dtp* gene. (**A**) Schematic of the zebrafish *dtp* locus. The nearest polymorphic markers are indicated, with corresponding numbers of recombinants and calculated genetic distances. (**B**) Deduced amino acid sequence near the *ahcy* mutation identified in *dtp* larvae (indicated in red; DR, *Danio rerio*), with corresponding amino acid sequence of orthologous Ahcy proteins from *Homo sapiens* (HS), *Xenopus laevis* (XL), *Drosophila melanogaster* (DM) and *Roseobacter*. (**C**) Schematic of the methionine metabolism pathway. Reduced Ahcy activity is predicted to increase levels of SAH, which inhibits methyltransferases. (**D-G**) *ahcy* expression in staged zebrafish embryos and larvae. Ubiquitous expression is evident through 24 hpf. Expression at 48 hpf and 72 hpf is restricted to the liver (yellow arrow), intestine (green arrow) and pancreas (blue arrow). (**H**) Immunostaining at sphere stage, showing ubiquitous immunoreactive Ahcy protein.

(Fig. 3A,B, red lines), while the SAM:SAH ratio was reduced. Elevated SAM associated with Ahcy inhibition has been reported previously, and is thought to be secondary to reduced SAM utilization associated with SAH-mediated inhibition of methyltransferases (Chiang et al., 1996). The elevated SAH and SAM levels and the reduced SAM:SAH ratio in 2-dpf *dtp* mutants were rescued by injection of mRNA encoding wild-type, but not *dtp*, Ahcy protein, confirming that the mutant Ahcy is either inactive or has greatly reduced activity (Fig. 3C,D). Microinjected *ahcy* mRNA did not rescue the methionine metabolism defect, hepatic steatosis or hepatic degeneration of 5-dpf *dtp* larvae when injected into 1-cell stage embryos or the yolk at 2 dpf (data not shown), most likely because of the short half-life of the mRNA.

To directly examine the effects of the *dtp* mutation on methylation, we assayed global DNA methylation and global lysine methylation in tissue from mutant larvae enriched for liver. Both DNA and lysine methylation, as measured by anti-methylcytosine and anti-methyl-lysine immunoblots, were decreased in *dtp*, a finding consistent with a global inhibition of methylation caused by elevated SAH or decreased SAM:SAH (Fig. 3E,F). The effect of elevated SAH on lipid methylation was determined by measuring the ratio of phosphatidylethanolamine (PE) to its methylation product phosphatidylcholine (PC) in *dtp* mutants. Although elevated SAH is predicted to inhibit the activity of phosphatidylethanolamine methyltransferase (Pemt), the hepatic enzyme responsible for the metabolic conversion of PE to PC, the ratio of these two metabolites was normal (see Fig. S2 in the supplementary material), most likely because of the utilization of yolk-derived PC, or the synthesis of PC from yolk-derived choline via the Kennedy pathway [cytidine 5-diphospho (CDP)-choline pathway] (McMaster and Bell, 1997), rather than a lack of Pemt inhibition. This finding is important because a reduced PC:PE ratio causes severe steatohepatitis in mice (Zhu et al., 2003), and therefore it might be expected to be reduced in *dtp* mutants.

The expression of lipogenic genes, of genes responsive to oxidative stress and of *tnfa* is increased in *dtp* larvae

Microarray analyses have been used to identify gene expression patterns altered in patients and rodent models with hepatic steatosis (Chung et al., 2005; Deaciuc et al., 2004; Esfandiari et al., 2005; Younossi et al., 2005). These studies have reported changes in the expression of genes involved in lipid metabolism, inflammation and fibrosis, and in genes encoding cytokines and proteins activated in response to oxidative stress. We compared the expression of some of these genes in *dtp* mutants and their wild-type siblings using real-time quantitative PCR. As in the other steatosis models, we found elevated expression of the lipogenic genes *pparg* and *srebp1*, the reactive oxygen species (ROS)-responsive gene *gpx* and the cytokine *tnfa* (NM 212859.2) in *dtp* larvae, although the elevation of *srebp1* only approached statistical significance (Fig. 4A-C). Interestingly, *pparg* also functions as an anti-inflammatory gene, but its role in hepatic steatosis is likely to be related to its lipogenic functions. Expression of a second zebrafish *tnf* gene, *tnfb* (NM 1024447.1) was unchanged between wild type and *dtp* (data not shown). Western analysis confirmed a 3-fold elevation of Tnfα protein levels in *dtp* larvae (Fig. 4D) and whole-mount RNA in situ hybridization experiments showed increased *tnfa* expression in the liver, intestine and swim bladder of most *dtp* larvae examined (Fig. 4E,F).

Tnfα mediates hepatic steatosis and degeneration in *dtp* larvae

To assess the effect of elevated Tnfα in *dtp* mutants, we assayed the effect of *tnfa* knockdown induced by antisense morpholinos. Injection of a *tnfa* morpholino into the yolk of 2-dpf *dtp* larvae decreased Tnfα protein expression (Fig. 4E), demonstrating the effectiveness of morpholino-mediated knockdown at later embryonic stages, as previously reported (Stenkamp and Frey,

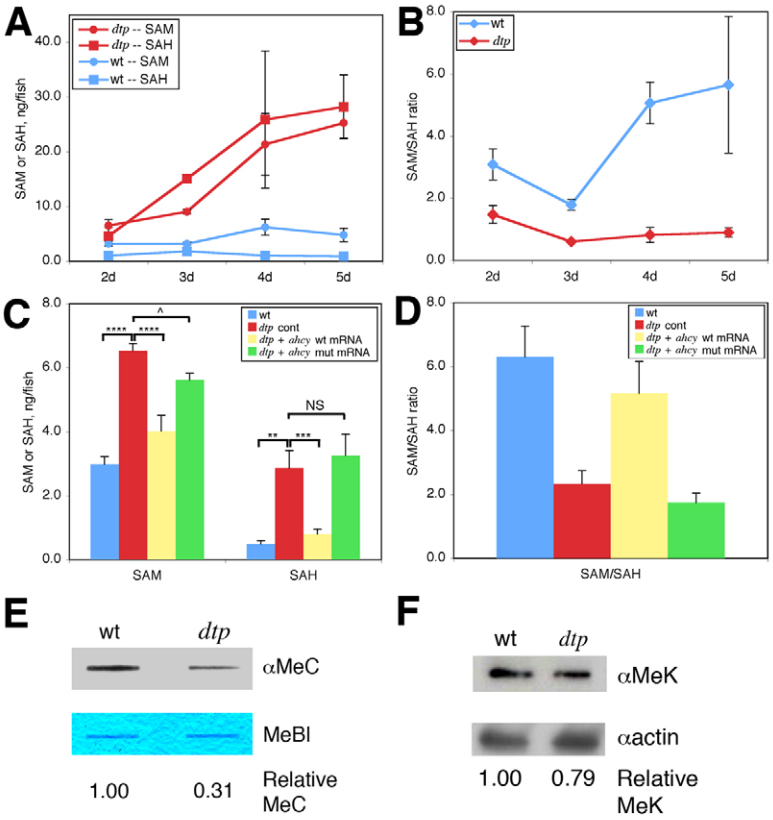

Fig. 3. Altered methionine and methyl metabolism in *dtp* larvae. (**A**) SAM and SAH levels, and (**B**) SAM:SAH ratio in wild-type (wt) and *dtp* zebrafish larvae. (**C**) SAM and SAH levels in 2-dpf wild-type and *dtp* embryos injected with control morpholino (*dtp* cont), and *dtp* embryos injected with either wild-type *ahcy* mRNA or mRNA carrying the *ahcy*^{dtp} missense mutation. ****P<0.00001, ***P<0.0001, **P<0.01, ^P<0.05; NS, not significant (P=0.3). (**D**) Calculated SAM:SAH ratio for the four conditions in C. Differences in the SAM:SAH ratio between B and D arise from experimental variation. (**E**) Anti-methylcytosine (αMeC) slot blot of genomic DNA derived from wild-type or *dtp* larvae, with Methylene Blue counterstain (MeBl). (**F**) Western blot showing reduced levels of methylated lysine residues (αMeK) in protein from *dtp* larvae; actin provided a loading control (αactin).

2003). The livers of the morpholino-injected *dtp* larvae were significantly larger than those of sibling *dtp* mutants injected with vehicle control (Fig. 4H,I), and the histological appearance of the hepatocytes more closely resembled wild-type hepatocytes, thus confirming rescue of the hepatic phenotype [Fig. 4J,K; rescue was present in 13 of 17 genotyped *dtp*$^{-/-}$ larvae analyzed by *transferrin a* (*tfa*) in situ or tissue staining]. Ultrastructural analysis showed reduced steatosis in the hepatocytes of morpholino-injected *dtp* larvae and an improvement in the appearance of the mitochondria (Fig. 4L). Injection of *tnfa* morpholino into wild-type larvae had no effect on liver size, histology or ultrastructure (data not shown). These data confirm a central role for Tnfα in the *dtp* phenotype.

tnfa expression, hepatic steatosis and degeneration persist in gnotobiotic *dtp* larvae

TNF expression is activated in hepatic macrophages (Kupffer cells) and circulating mononuclear cells in patients with alcoholic liver disease and non-alcoholic steatohepatitis (Hoek and Pastorino, 2002; Tomita et al., 2006). The gut microbiota is believed to activate *TNF* in these cells (Thakur et al., 2007). To determine whether an innate immune response to endotoxin derived from Gram-negative gut bacteria plays a role in the *dtp* mutant phenotype, we measured *tnfa* gene expression and liver morphology in *dtp* larvae reared under germ-free conditions (Rawls et al., 2004; Bates et al., 2006). *tnfa* expression remained elevated in gnotobiotic *dtp* larvae and the hepatic phenotype appeared unchanged, based on *tfa* RNA in situ hybridization (see Fig. S3 in the supplementary material) and histology (not shown).

Having excluded a role for the gut microbiota in *tnfa* activation, we sought to determine whether reduced DNA methylation at *tnfa* regulatory elements could account for increased Tnfα levels in *dtp* mutants. We treated zebrafish larvae with 5-azacytidine (azaC), a nucleoside analog that reversibly inhibits DNA methyltransferases (Jones and Taylor, 1980). AzaC treatment inhibits methylation of hemimethylated cytidine residues in the DNA of replicating cells. Surprisingly, azaC injection into the yolk of 2- to 4-dpf zebrafish had little effect on larval morphology, even though DNA methylation levels were halved (see Fig. S4 in the supplementary material). In addition to their normal gross liver morphology, histological analysis of the azaC-injected larvae revealed no evidence of hepatic steatosis or of liver degeneration, nor was there any ultrastructural evidence of mitochondrial defects (see Fig. S4 in the supplementary material). Furthermore, quantitative RT-PCR showed no increase in *tnfa* expression in azaC-treated larvae (see Fig. S4 in the supplementary material). Finally, analysis of *tnfa* regulatory elements within 4 kb upstream to 1 kb downstream of the transcription start site did not identify any CpG islands (Sanger Centre zebrfish genome sequence version 7.0; data not shown). Together, these data argue against the idea that elevated *tnfa* levels in *dtp* larva arise from reduced DNA methylation at *tnfa* regulatory elements.

Steatosis and reduced mitochondrial antioxidants in adult zebrafish treated with the Ahcy inhibitor 3-deaza-adenosine

Mitochondrial glutathione (mGSH) acts as a scavenger of ROS, and depletion of mGSH is associated with several models of hepatic steatosis and steatohepatitis (Garcia-Ruiz and Fernandez-Checa, 2006). mGSH depletion also sensitizes hepatocytes to injury and cell death caused by TNFα (Mari et al., 2006). Given that the ultrastructural analyses suggest mitochondrial dysfunction in *dtp* hepatocytes, we attempted to measure mGSH levels in liver mitochondria derived from *dtp* larvae. Reduced liver size limited the recovery of sufficient mitochondria to perform this assay. A

sufficient number of liver mitochondria were however recovered from adult zebrafish treated with the Ahcy inhibitor 3-deaza-adenosine (deazaA) (Guranowski et al., 1981). DeazaA treatment for 7 days increased liver *tnfa* expression and caused hepatic steatosis (Fig. 5). Although these fish had only mild hepatocyte mitochondrial ultrastructural defects (data not shown), a modest yet highly significant reduction of mGSH was evident (Fig. 5D).

Despite causing steatosis and mitochondrial dysfunction, deazaA treatment had only a modest effect on methionine metabolism, as liver SAH levels were unchanged and SAM levels were elevated in these fish (Fig. 6A). Homocysteine levels, however, were reduced following 7 days of deazaA treatment, supporting reduced Ahcy function (5.62±1.89 ng/mg liver in untreated fish versus 2.89±1.08 in treated fish; P=0.03). The levels of SAM and SAH in the livers of heterozygous adult male *dtp* fish were similar to those in the deazaA-treated livers (Fig. 6B). These metabolic defects were interesting because although mild steatosis was present in deazaA-treated adult fish, pronounced hepatic steatosis was evident in all of the adult male heterozygous *dtp* fish we examined (Fig. 6C-F) (n=11). *tnfa* expression was modestly increased in the liver of adult heterozygous *dtp* fish (Fig. 6G), similar to that in the adult fish treated with deazaA. Furthermore, adult *dtp* heterozygotes demonstrated elevated expression of *pparg* (Fig. 6H) and of the ROS-sensitive gene *trx* (Fig. 6I), similar to that in homozygous larvae and consistent with other models of hepatic steatosis (Chung et al., 2005; Deaciuc et al., 2004; Esfandiari et al., 2005; Younossi et al., 2005). In contrast to heterozygous adults, hepatic steatosis was not detected in 5-dpf heterozygous *dtp* larvae (not shown).

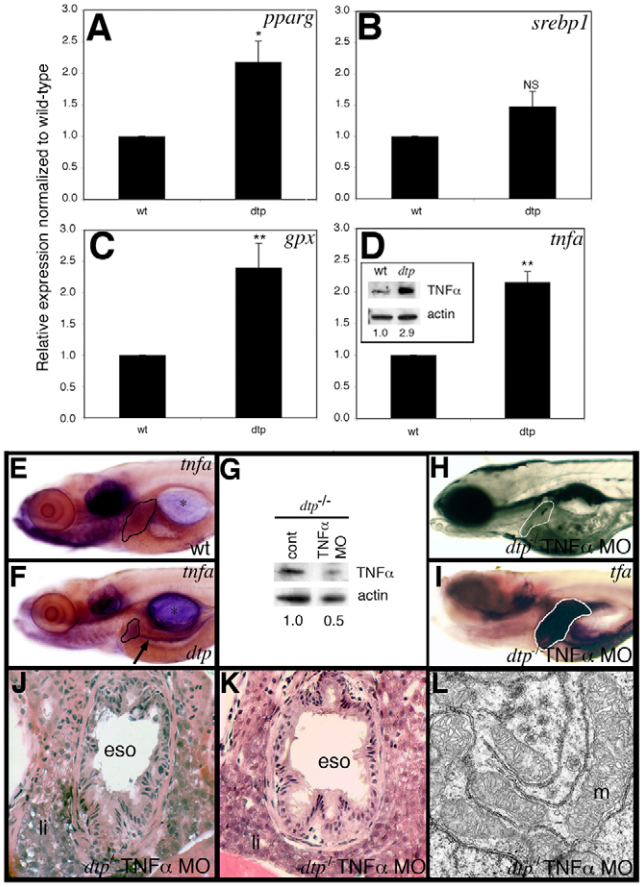

Fig. 4. Increased expression of lipogenic and stress-responsive genes in *dtp* larvae, and rescue of *dtp* steatosis and liver degeneration with *tnfa* knockdown. (**A-D**) Expression levels of *peroxisome proliferator-activated receptor gamma* (*pparg*, A), *sterol response element binding protein 1* (*srebp1*, B), *glutathione peroxidase* (*gpx*, C) and *tumor necrosis factor alpha* (*tnfa*, D) in 4-dpf *dtp* versus wild-type (wt) siblings. Inset for D shows Tnfα western blot in 5-dpf *dtp* larvae. **P*<0.05, ***P*<0.005; NS, not significant (*P*=0.07). (**E**,**F**) Whole-mount RNA in situ hybridization showing enhanced *tnfa* expression in the liver (outlined), intestine (arrow) and swim bladder (*) of a *dtp* larva (F) as compared with a wild-type sibling (E). (**G**) Western blot showing reduced Tnfα protein in *tnfa* morpholino-injected larvae. (**H**) Lateral view of a fixed 5-dpf *dtp* larva injected with *tnfa* antisense morpholino oligonucleotide at 2 dpf; liver size is enlarged (outlined), compare with live *dtp* 5-dpf larva depicted in Fig. 1. (**I**) Liver rescue in *tnfa* morpholino-injected *dtp* mutant as revealed by *transferrin* (*tfa*) in situ hybridization. (**J**,**K**) *tnfa* knockdown also rescues *dtp* liver histology (compare with Fig. 1J). (**L**) Mitochondrial ultrastructure is improved and steatosis is rescued by *tnfa* knockdown. eso, esophagus; li, liver; m, mitochondria.

DISCUSSION

Causative loss-of-function mutation of *ahcy* in zebrafish *dtp* mutants

In this report we describe the hepatic phenotype associated with a loss-of-function mutation of the gene encoding zebrafish S-adenosylhomocysteine hydrolase (Ahcy), a methionine metabolism enzyme that is highly conserved in prokaryotes and eukaryotes. These data complement previously published studies showing the

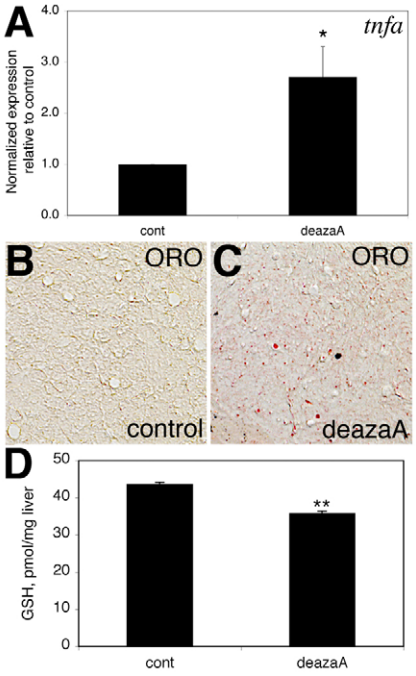

Fig. 5. Ahcy inhibition in adult zebrafish causes liver steatosis and activates *tnfa* expression. (**A**) Quantitative real-time PCR reveals elevated *tnfa* expression in adult zebrafish liver following 7-day treatment with the Ahcy inhibitor 3-deaza-adenosine (deazaA). (**B**,**C**) Oil Red O staining reveals steatosis in deazaA-treated adult livers, as compared with control. (**D**) Reduced liver mitochondrial glutathione (GSH) in deazaA-treated adult fish compared with control. **P*<0.05, ***P*<0.005; error bars indicate s.e.m.

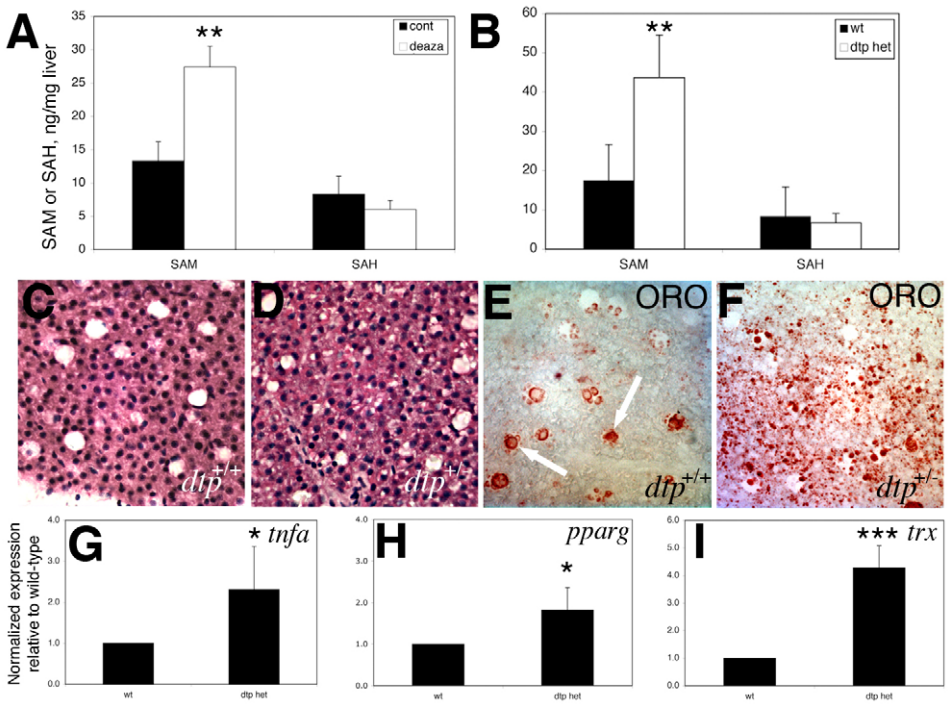

Fig. 6. Liver steatosis, increased lipogenic gene expression, and methionine metabolism defects in adult *dtp* heterozygotes. (**A**,**B**) SAM and SAH levels from livers of (A) adult fish treated with deazaA and (B) adult *dtp* heterozygotes, as compared with wild-type (wt) controls. (**C**,**D**) Liver histology from adult wild-type and heterozygous *dtp* fish showing vesicular clearing consistent with steatosis. (**E**,**F**) Oil Red O staining of adult wild-type and heterozygous *dtp* fish reveals steatosis in the heterozygotes. Lipid is evident in wild-type liver sinusoids (E, arrows), but not in hepatocytes. (**G-I**) Elevated expression of *tnfa* (G), *pparg* (H) and the ROS-sensitive gene *thioredoxin reductase* (*trx*) (I), in the liver of adult *dtp* heterozygous versus wild-type fish. **P*=0.05, ***P*<0.05, ****P*<0.005.

effect of this mutation on the proliferation and survival of exocrine pancreas progenitor cells in zebrafish *dtp* mutant larvae (Yee et al., 2005). Multiple lines of evidence described in this report support the identification of *ahcy* as the *dtp* gene. These include tight genetic linkage, mutation of a highly conserved methionine residue in a functional domain of the Ahcy protein, altered levels of methionine metabolites that were not rescued by $ahcy^{dtp}$ mRNA injections (indicating reduced function of the *dtp* Ahcy protein), and partial phenocopy of *dtp* by *ahcy* knockdown and Ahcy inhibition. In addition to these findings, no mutations were identified in the coding regions of other genes in the critical interval surrounding the *dtp* locus.

Comparable methionine metabolism defects in *dtp* larvae and chronic liver disease patients

Methionine metabolism is disrupted in patients with alcoholic liver disease and other chronic liver conditions, and there is strong experimental evidence linking such defects to the development of steatosis that can progress to cirrhosis, liver failure and liver cancer (Kharbanda, 2007). SAM depletion and/or a reduced SAM:SAH ratio are important consequences of altered methionine metabolism, as evidenced by the ability of SAM or its metabolic precursor, betaine, to delay disease progression in animal liver disease models and in patients with alcoholic liver disease (Lu et al., 2001; Villanueva and Halsted, 2004). SAM depletion in chronic liver conditions arises from nutritional deficiencies coupled with reduced activity of the methionine metabolism enzyme methionine synthase (MAT1A) and reduced *BHMT* gene expression (Kharbanda, 2007; Lu et al., 2002). This reduces SAM synthesis, elevates cellular SAH (because hydrolysis of SAH by Ahcy is reversible), and reduces the SAM:SAH ratio. By contrast, SAM and SAH are both elevated in *dtp*, but the SAM:SAH ratio is reduced because the rise in SAM is proportionately less than that in SAH. Increased SAH in *dtp* is a direct effect of reduced Ahcy activity, whereas SAM levels increase in *dtp* because of SAH-mediated inhibition of methyltransferases.

Association of methionine metabolism defects, mitochondrial dysfunction and changes in methylation potential in *dtp* mutants

Regardless of the cause, methionine metabolism defects induce a complex set of cellular responses that disrupt hepatocyte lipid metabolism and, in some instances, activate apoptotic or non-apoptotic cell death pathways. Mitochondrial dysfunction is one of the more commonly reported defects. Cytosolic SAM is imported into mitochondria by a specific transporter that is inhibited by high levels of cytosolic SAH (Agrimi et al., 2004; Horne et al., 1997; Song et al., 2007). Reduced mitochondrial SAM caused by elevated SAH is predicted to disrupt mitochondrial function through a variety of mechanisms arising from altered methylation potential [discussed by Song et al. (Song et al., 2007)]. Although the transporter that imports GSH into mitochondria has not been identified, it is known that reduced SAM:SAH alters mitochondrial membrane fluidity (Colell et al., 1997), thereby disrupting the import of GSH, an important antioxidant. Reduced mGSH leads to the oxidation of mitochondrial proteins, lipid and DNA by ROS that are normally quenched by GSH. These oxidative modifications cause mitochondrial dysfunction, which in turn increases ROS production and causes further mitochondrial damage. Ultimately, this decreases hepatocyte lipid utilization, which contributes to steatosis.

Although we did not directly assess the effect of elevated SAH on mitochondrial SAM transport, several lines of evidence show that mitochondrial dysfunction is important to the development of liver steatosis and degeneration in *dtp* mutants. First, all homozygous *dtp* larvae had pronounced liver mitochondrial ultrastructural defects. Second, mGSH levels were reduced in the liver of deazaA-treated adult fish that had steatosis. Third, mitochondrial ultrastructure improved in *dtp* larvae rescued by *tnfa* knockdown. The latter finding is noteworthy because TNFα inhibition improves mitochondrial function in mammalian steatosis models (Garcia-Ruiz et al., 2006).

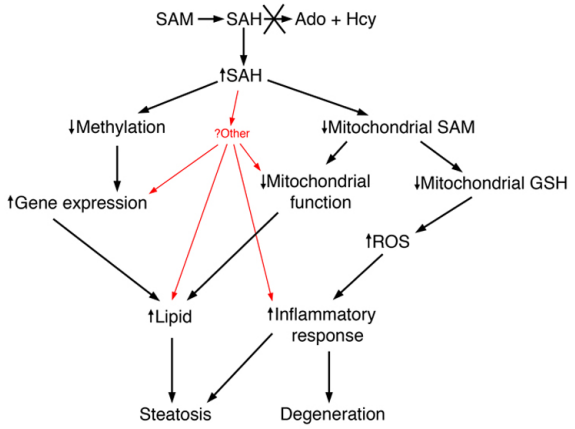

Fig. 7. Mechanistic model of hepatic steatosis and liver degeneration caused by Ahcy deficiency. Mutation of *ahcy* disrupts Ahcy activity, increasing cellular SAH. This alters mitochondrial function and reduces cellular methylation potential, thereby altering the expression of lipogenic genes such as *tnfa* and *pparg*, possibly through an epigenetic mechanism involving alteration of the histone methylation code. This leads to enhanced lipid synthesis, reduced lipid utilization and, possibly, enhanced lipid uptake, as well as to the sensitization of hepatocytes to TNFα-induced cell death. Additional, as yet unidentified effects of altered SAH or altered methylation potential might also play a mechanistic role in the *dtp* phenotype.

In addition to causing mitochondrial dysfunction, methionine metabolism defects are predicted to alter total cellular methylation potential, as a reduced SAM:SAH ratio and/or elevated SAH inhibit a wide range of cytosolic and nuclear methyltransferases (Chiang et al., 1996). Up to 75% of all mammalian transmethylation reactions occur in the liver (Xue and Snoswell, 1986), and elevated liver SAH has been shown to inhibit the methylation of histones, DNA and lipids in a dose-dependent fashion (Duerre and Briske-Anderson, 1981). *Mat1*, *Pemt* and *Gnmt* knockout mice all develop steatosis, as do human patients with GNMT deficiency (Li et al., 2006; Lu et al., 2001; Luka et al., 2006; Martinez-Chantar et al., 2008; Zhu et al., 2003). Elevated SAH also causes steatosis and liver degeneration in murine adenosine kinase deficiency [a model of neonatal hepatitis (Boison et al., 2002)]. Together, these data suggest that the *dtp* liver phenotype is caused by reduced methylation potential. This is likely to arise from a combined effect on mitochondrial function and, as discussed below, of enhanced *tnfa* expression.

dtp may be used to model TNFα-induced hepatic steatosis and liver degeneration

The role of TNFα in hepatic steatosis is well established. Serum TNFα is increased in patients with chronic and acute liver failure (Felver et al., 1990; Manco et al., 2007; Streetz et al., 2000) and anti-TNFα treatment rescues hepatic steatosis and inflammation in animal models (Barbuio et al., 2007; Endo et al., 2007; Garcia-Ruiz et al., 2006; Koca et al., 2007). TNFα can disrupt lipid metabolism through a variety of mechanisms including perturbation of mitochondrial function (Anstee and Goldin, 2006; Garcia-Ruiz et al., 2006), activation of lipogenic gene expression, and enhanced uptake of circulating lipid by the liver (reviewed by Anstee and Goldin, 2006). TNFα can also induce hepatocyte cell death, particularly in the setting of mitochondrial dysfunction, such as that caused by elevated SAH (Anstee and Goldin, 2006; Bradham et al., 1998; Garcia-Ruiz et al., 2003; Garcia-Ruiz and Fernandez-Checa, 2006; Song et al., 2004). Our data point to an effect of Tnfα on mitochondrial function, hepatocyte degeneration and, possibly, lipogenic gene expression in *dtp* mutants. We speculate that Tnfα might also enhance the uptake of yolk-derived lipid in *dtp* larvae.

Given the importance of TNFα in mammalian steatosis, we were interested in identifying the stimulus that activates *tnfa* expression in *dtp*. Reduced clearance of gut bacteria that enter the portal circulation, coupled with enhanced sensitivity to endotoxin derived from these resident microbiota, are considered the principal mechanisms of *TNF* activation in patients with alcoholic liver disease and NASH (Bode and Bode, 2005; Mathurin et al., 2000; Wigg et al., 2001). *ahcy* is strongly expressed in the intestine of zebrafish larvae, and for this reason we initially thought that altered permeability of the intestinal epithelium to the gut microbiota might activate *tnfa* expression in *dtp* mutants. However, *tnfa* expression was unchanged in gnotobiotic *dtp* larvae, indicating that there was a different cause for the enhanced expression.

Because of the known effects of Ahcy inhibition on methylation, we speculated that an epigenetic mechanism, such as reduced DNA methylation at the *tnfa* or another gene locus, could activate *tnfa* expression in *dtp*, such as occurs during hematopoietic stem cell differentiation (Sullivan et al., 2007). However, our analysis of the putative *tnfa* promoter region in the zebrafish genome database did not identify any CpG islands, and reduced DNA methylation caused by azaC did not activate *tnfa* expression in zebrafish larvae. Thus, we considered changes in DNA methylation an unlikely cause of enhanced *tnfa* expression.

Global methylated lysine was also reduced in *dtp*, raising the possibility that changes in histone methylation might epigenetically activate *tnfa* expression. Supporting this idea, reduced levels of the inhibitory mark dimethyl-H3K9 correlate with increased *TNF* expression in endotoxin-stimulated human mononuclear cells (El Gazzar et al., 2007). A reduction in the number of inhibitory trimethyl-H3K27 marks also correlates with activation of gene expression during development, differentiation and response to immune stimuli (Agger et al., 2007; Cloos et al., 2008; Jepsen et al., 2007; Lan et al., 2007). In contrast to these studies suggesting that *tnfa* expression can be activated by the removal of inhibitory methyl marks, Ara and colleagues recently reported that lipopolysaccharide-induced activation of *Tnf* expression in mouse macrophages is associated with increased levels of an activating methyl mark, trimethyl-H3K4, and that this was inhibited by SAH (Ara et al., 2008). We speculate that these conflicting data are likely to be attributable to stimulus- and cell type-dependent changes in methylation potential, and that Ahcy inhibition in *dtp* alters the balance between methylation and demethylation of histone H3 lysine residues associated with the *tnfa* promoter, or *tnfa* regulatory loci, in liver mononuclear immune cells (Kupffer cells), or possibly even hepatocytes, as suggested by the *tnfa* expression pattern in *dtp* larvae. Consistent with this model, pharmacological inhibition of Ahcy causes cell type-specific changes in gene expression in cancer cells and T-cell subsets (Lawson et al., 2007; Tan et al., 2007). A related epigenetic mechanism of gene regulation has also been reported in mouse ES cells (Pasini et al., 2008).

In summary, extensive evidence from human liver disease patients, animal liver disease models and in vitro systems indicates a causative role for altered methionine metabolism in steatosis, steatohepatitis and liver degeneration. Our analyses of *dtp* mutants, adult heterozygous *dtp* fish and adult fish treated with the Ahcy inhibitor deazaA extend these observations to zebrafish. As summarized in Fig. 7, our data suggest that *tnfa* overexpression and mitochondrial dysfunction are

the principal causes of the *dtp* liver phenotype. This model of TNFα-mediated steatosis is novel as there are no previous reports of altered methylation potential activating *tnfa* gene expression. However, as pointed out in Fig. 7, we cannot exclude the possibility that other factors contribute to the *dtp* phenotype.

Relationship of the zebrafish and human Ahcy deficiency phenotypes

Clinical manifestations of human AHCY deficiency have been reported in only three patients (Baric et al., 2005; Baric et al., 2004; Buist et al., 2006). Motor and neurological defects were the prominent presenting symptoms in two siblings that are compound heterozygotes for two hypomorphic *AHCY* alleles. The first-identified patient also demonstrated biochemical hepatitis and mitochondrial abnormalities on liver biopsy at the age of 12 months (Baric et al., 2004), whereas the second patient had no demonstrable liver abnormalities, presumably because of an earlier diagnosis at age 3 months (Baric et al., 2005). A third, 26-year-old patient had comparable motor and neurological symptoms, in addition to hepatic steatosis and mitochondrial abnormalities evident on liver electron micrographs (Buist et al., 2006). It is intriguing that within this group of three AHCY-deficient patients, there appears to be a progression of mild to moderate liver disease with age, similar to our findings with the *dtp* heterozygotes. By contrast, pronounced hepatic steatosis and degeneration in homozygous *dtp* larvae most likely result from the combined effect of more severe Ahcy deficiency coupled with the rapid rate of hepatic metabolism of yolk-derived lipid nutrients in zebrafish larvae.

Steatosis in *dtp* heterozygotes suggest that *AHCY* polymorphisms might be heritable risk factors for steatosis in liver disease patients

Although heterozygous *dtp* larvae are indistinguishable from homozygous wild-type siblings and develop normally with no apparent reduction in fecundity or lifespan, as adults these fish develop pronounced hepatic steatosis. Surprisingly, liver SAH levels were not significantly elevated and SAM levels were elevated ~2-fold, raising the SAM:SAH ratio in these fish. Comparable SAM and SAH levels were noted in deazaA-treated adult fish that also developed steatosis. These findings were unexpected, as reduced Ahcy activity is expected to increase SAH levels and decrease the SAM:SAH ratio. We speculate that these biochemical findings result from either variable sensitivity of hepatic methyltransferases to SAH or increasing metabolism of homocysteine via betaine homocysteine methyltransferase (Bhmt) (see Fig. S5 in the supplementary material).

Regardless of the mechanism that accounts for the observed SAM and SAH levels in *dtp* heterozygous and deazaA-treated adult fish, hepatic steatosis in these fish raises the question of whether human *AHCY* polymorphisms that have only mild effects on methionine metabolism might be a risk factor for the development of steatosis associated with obesity, alcohol consumption and other conditions, such as chronic hepatitis C infection or drug-induced steatosis. Polymorphisms in the methionine metabolism gene *MTHFR* and hyperhomocysteinemia have been reported to promote steatosis and fibrosis in chronic hepatitis C patients (Adinolfi et al., 2005), and human *AHCY* polymorphisms that alter protein thermostability have already been described (Fumic et al., 2007). Given the potentially beneficial effects of AHCY inhibitors in treating cancer and autoimmune diseases (Hermes et al., 2008; Lawson et al., 2007; Tan et al., 2007), the population of patients that may benefit from *AHCY* genotyping could increase significantly in the near future. Molecular analysis of other zebrafish mutations that cause hepatic steatosis (Sadler et al., 2005) might identify additional heritable risk factors.

We thank Mani Muthimani, Erin Smith, Liyuan Ma, Steven EauClaire and Louis Capecci for excellent technical assistance, Dr Pierre Russo for help in interpretation of electron micrographs, and Dr Shelly Lu for helpful discussions. This work was supported by NIH grants K08 DK068009 (R.P.M.), R01 CA95586 and P30 ES013508 (I.A.B.), R03 AGO27893 (I.V.J.M.), and R01 DK61142 (M.P.), and by generous support from the Fred and Suzanne Biesecker Pediatric Liver Center at The Children's Hospital of Philadelphia. Deposited in PMC for release after 12 months.

Supplementary material

Supplementary material for this article is available at http://dev.biologists.org/cgi/content/full/136/5/865/DC1

References

Adinolfi, L. E., Ingrosso, D., Cesaro, G., Cimmino, A., D'Anto, M., Capasso, R., Zappia, V. and Ruggiero, G. (2005). Hyperhomocysteinemia and the MTHFR C677T polymorphism promote steatosis and fibrosis in chronic hepatitis C patients. *Hepatology* **41**, 995-1003.

Agger, K., Cloos, P. A., Christensen, J., Pasini, D., Rose, S., Rappsilber, J., Issaeva, I., Canaani, E., Salcini, A. E. and Helin, K. (2007). UTX and JMJD3 are histone H3K27 demethylases involved in HOX gene regulation and development. *Nature* **449**, 731-734.

Agrimi, G., Di Noia, M. A., Marobbio, C. M., Fiermonte, G., Lasorsa, F. M. and Palmieri, F. (2004). Identification of the human mitochondrial S-adenosylmethionine transporter: bacterial expression, reconstitution, functional characterization and tissue distribution. *Biochem. J.* **379**, 183-190.

Anstee, Q. M. and Goldin, R. D. (2006). Mouse models in non-alcoholic fatty liver disease and steatohepatitis research. *Int. J. Exp. Pathol.* **87**, 1-16.

Ara, A. I., Xia, M., Ramani, K., Mato, J. M. and Lu, S. C. (2008). S-adenosylmethionine inhibits lipopolysaccharide-induced gene expression via modulation of histone methylation. *Hepatology* **47**, 1655-1666.

Barbuio, R., Milanski, M., Bertolo, M. B., Saad, M. J. and Velloso, L. A. (2007). Infliximab reverses steatosis and improves insulin signal transduction in liver of rats fed a high-fat diet. *J. Endocrinol.* **194**, 539-550.

Baric, I., Fumic, K., Glenn, B., Cuk, M., Schulze, A., Finkelstein, J. D., James, S. J., Mejaski-Bosnjak, V., Pazanin, L., Pogribny, I. P. et al. (2004). S-adenosylhomocysteine hydrolase deficiency in a human: a genetic disorder of methionine metabolism. *Proc. Natl. Acad. Sci. USA* **101**, 4234-4239.

Baric, I., Cuk, M., Fumic, K., Vugrek, O., Allen, R. H., Glenn, B., Maradin, M., Pazanin, L., Pogribny, I., Rados, M. et al. (2005). S-Adenosylhomocysteine hydrolase deficiency: a second patient, the younger brother of the index patient, and outcomes during therapy. *J. Inherit. Metab. Dis.* **28**, 885-902.

Bates, J. M., Mittge, E., Kuhlman, J., Baden, K. N., Cheesman, S. E. and Guillemin, K. (2006). Distinct signals from the microbiota promote different aspects of zebrafish gut differentiation. *Dev. Biol.* **297**, 374-386.

Bode, C. and Bode, J. C. (2005). Activation of the innate immune system and alcoholic liver disease: effects of ethanol per se or enhanced intestinal translocation of bacterial toxins induced by ethanol? *Alcohol Clin. Exp. Res.* **29**, 166S-171S.

Boison, D., Scheurer, L., Zumsteg, V., Rulicke, T., Litynski, P., Fowler, B., Brandner, S. and Mohler, H. (2002). Neonatal hepatic steatosis by disruption of the adenosine kinase gene. *Proc. Natl. Acad. Sci. USA* **99**, 6985-6990.

Bradham, C. A., Qian, T., Streetz, K., Trautwein, C., Brenner, D. A. and Lemasters, J. J. (1998). The mitochondrial permeability transition is required for tumor necrosis factor alpha-mediated apoptosis and cytochrome c release. *Mol. Cell. Biol.* **18**, 6353-6364.

Browning, J. D. and Horton, J. D. (2004). Molecular mediators of hepatic steatosis and liver injury. *J. Clin. Invest.* **114**, 147-152.

Buist, N. R., Glenn, B., Vugrek, O., Wagner, C., Stabler, S., Allen, R. H., Pogribny, I., Schulze, A., Zeisel, S. H., Baric, I. et al. (2006). S-adenosylhomocysteine hydrolase deficiency in a 26-year-old man. *J. Inherit. Metab. Dis.* **29**, 538-545.

Chiang, P. K. (1998). Biological effects of inhibitors of S-adenosylhomocysteine hydrolase. *Pharmacol. Ther.* **77**, 115-134.

Chiang, P. K., Gordon, R. K., Tal, J., Zeng, G. C., Doctor, B. P., Pardhasaradhi, K. and McCann, P. P. (1996). S-Adenosylmethionine and methylation. *FASEB J.* **10**, 471-480.

Chung, H., Hong, D. P., Kim, H. J., Jang, K. S., Shin, D. M., Ahn, J. I., Lee, Y. S. and Kong, G. (2005). Differential gene expression profiles in the steatosis/fibrosis model of rat liver by chronic administration of carbon tetrachloride. *Toxicol. Appl. Pharmacol.* **208**, 242-254.

Cloos, P. A., Christensen, J., Agger, K. and Helin, K. (2008). Erasing the methyl mark: histone demethylases at the center of cellular differentiation and disease. *Genes Dev.* **22**, 1115-1140.

Colell, A., Garcia-Ruiz, C., Morales, A., Ballesta, A., Ookhtens, M., Rodes, J., Kaplowitz, N. and Fernandez-Checa, J. C. (1997). Transport of reduced glutathione in hepatic mitochondria and mitoplasts from ethanol-treated rats: effect of membrane physical properties and S-adenosyl-L-methionine. *Hepatology* **26**, 699-708.
Deaciuc, I. V., Doherty, D. E., Burikhanov, R., Lee, E. Y., Stromberg, A. J., Peng, X. and de Villiers, W. J. (2004). Large-scale gene profiling of the liver in a mouse model of chronic, intragastric ethanol infusion. *J. Hepatol.* **40**, 219-227.
Diehl, A. M. (2005). Lessons from animal models of NASH. *Hepatol. Res.* **33**, 138-144.
Duerre, J. A. and Briske-Anderson, M. (1981). Effect of adenosine metabolites on methyltransferase reactions in isolated rat livers. *Biochim. Biophys. Acta* **678**, 275-282.
Duong, F. H., Christen, V., Filipowicz, M. and Heim, M. H. (2006). S-Adenosylmethionine and betaine correct hepatitis C virus induced inhibition of interferon signaling *in vitro*. *Hepatology* **43**, 796-806.
El Gazzar, M., Yoza, B. K., Hu, J. Y., Cousart, S. L. and McCall, C. E. (2007). Epigenetic silencing of tumor necrosis factor alpha during endotoxin tolerance. *J. Biol. Chem.* **282**, 26857-26864.
Endo, M., Masaki, T., Seike, M. and Yoshimatsu, H. (2007). TNF-alpha induces hepatic steatosis in mice by enhancing gene expression of sterol regulatory element binding protein-1c (SREBP-1c). *Exp. Biol. Med.* **232**, 614-621.
Esfandiari, F., Villanueva, J. A., Wong, D. H., French, S. W. and Halsted, C. H. (2005). Chronic ethanol feeding and folate deficiency activate hepatic endoplasmic reticulum stress pathway in micropigs. *Am. J. Physiol. Gastrointest. Liver Physiol.* **289**, G54-G63.
Felver, M. E., Mezey, E., McGuire, M., Mitchell, M. C., Herlong, H. F., Veech, G. A. and Veech, R. L. (1990). Plasma tumor necrosis factor alpha predicts decreased long-term survival in severe alcoholic hepatitis. *Alcohol Clin. Exp. Res.* **14**, 255-259.
Fromenty, B., Robin, M. A., Igoudjil, A., Mansouri, A. and Pessayre, D. (2004). The ins and outs of mitochondrial dysfunction in NASH. *Diabetes Metab.* **30**, 121-138.
Fumic, K., Beluzic, R., Cuk, M., Pavkov, T., Kloor, D., Baric, I., Mijic, I. and Vugrek, O. (2007). Functional analysis of human S-adenosylhomocysteine hydrolase isoforms SAHH-2 and SAHH-3. *Eur. J. Hum. Genet.* **15**, 347-351.
Garcia-Ruiz, C. and Fernandez-Checa, J. C. (2006). Mitochondrial glutathione: hepatocellular survival-death switch. *J. Gastroenterol. Hepatol.* **21 Suppl. 3**, S3-S6.
Garcia-Ruiz, C., Colell, A., Mari, M., Morales, A., Calvo, M., Enrich, C. and Fernandez-Checa, J. C. (2003). Defective TNF-alpha-mediated hepatocellular apoptosis and liver damage in acidic sphingomyelinase knockout mice. *J. Clin. Invest.* **111**, 197-208.
Garcia-Ruiz, I., Rodriguez-Juan, C., Diaz-Sanjuan, T., del Hoyo, P., Colina, F., Munoz-Yague, T. and Solis-Herruzo, J. A. (2006). Uric acid and anti-TNF antibody improve mitochondrial dysfunction in ob/ob mice. *Hepatology* **44**, 581-591.
Guranowski, A., Montgomery, J. A., Cantoni, G. L. and Chiang, P. K. (1981). Adenosine analogues as substrates and inhibitors of S-adenosylhomocysteine hydrolase. *Biochemistry* **20**, 110-115.
Hermes, M., Geisler, H., Osswald, H., Riehle, R. and Kloor, D. (2008). Alterations in S-adenosylhomocysteine metabolism decrease O6-methylguanine DNA methyltransferase gene expression without affecting promoter methylation. *Biochem. Pharmacol.* **75**, 2100-2111.
Hoek, J. B. and Pastorino, J. G. (2002). Ethanol, oxidative stress, and cytokine-induced liver cell injury. *Alcohol* **27**, 63-68.
Horne, D. W., Holloway, R. S. and Wagner, C. (1997). Transport of S-adenosylmethionine in isolated rat liver mitochondria. *Arch. Biochem. Biophys.* **343**, 201-206.
Hu, Y., Komoto, J., Huang, Y., Gomi, T., Ogawa, H., Takata, Y., Fujioka, M. and Takusagawa, F. (1999). Crystal structure of S-adenosylhomocysteine hydrolase from rat liver. *Biochemistry* **38**, 8323-8333.
Hu, Y., Yang, X., Yin, D. H., Mahadevan, J., Kuczera, K., Schowen, R. L. and Borchardt, R. T. (2001). Computational characterization of substrate binding and catalysis in S-adenosylhomocysteine hydrolase. *Biochemistry* **40**, 15143-15152.
Innis, S. M. and Hasman, D. (2006). Evidence of choline depletion and reduced betaine and dimethylglycine with increased homocysteine in plasma of children with cystic fibrosis. *J. Nutr.* **136**, 2226-2231.
Jepsen, K., Solum, D., Zhou, T., McEvilly, R. J., Kim, H. J., Glass, C. K., Hermanson, O. and Rosenfeld, M. G. (2007). SMRT-mediated repression of an H3K27 demethylase in progression from neural stem cell to neuron. *Nature* **450**, 415-419.
Jones, P. A. and Taylor, S. M. (1980). Cellular differentiation, cytidine analogs and DNA methylation. *Cell* **20**, 85-93.
Kharbanda, K. K. (2007). Role of transmethylation reactions in alcoholic liver disease. *World J. Gastroenterol.* **13**, 4947-4954.
Koca, S. S., Bahcecioglu, I. H., Poyrazoglu, O. K., Ozercan, I. H., Sahin, K. and Ustundag, B. (2007). The treatment with antibody of TNF-alpha Reduces the inflammation, necrosis and fibrosis in the non-alcoholic steatohepatitis induced by methionine- and choline-deficient diet. *Inflammation* **31**, 91-98.
Lan, F., Bayliss, P. E., Rinn, J. L., Whetstine, J. R., Wang, J. K., Chen, S., Iwase, S., Alpatov, R., Issaeva, I., Canaani, E. et al. (2007). A histone H3 lysine 27 demethylase regulates animal posterior development. *Nature* **449**, 689-694.
Lawson, B. R., Manenkova, Y., Ahamed, J., Chen, X., Zou, J. P., Baccala, R., Theofilopoulos, A. N. and Yuan, C. (2007). Inhibition of transmethylation down-regulates CD4 T cell activation and curtails development of autoimmunity in a model system. *J. Immunol.* **178**, 5366-5374.
Li, Q. S., Cai, S., Borchardt, R. T., Fang, J., Kuczera, K., Middaugh, C. R. and Schowen, R. L. (2007). Comparative kinetics of cofactor association and dissociation for the human and trypanosomal S-adenosylhomocysteine hydrolases. 1. Basic features of the association and dissociation processes. *Biochemistry* **46**, 5798-5809.
Li, Z., Agellon, L. B., Allen, T. M., Umeda, M., Jewell, L., Mason, A. and Vance, D. E. (2006). The ratio of phosphatidylcholine to phosphatidylethanolamine influences membrane integrity and steatohepatitis. *Cell Metab.* **3**, 321-331.
Lorent, K., Yeo, S. Y., Oda, T., Chandrasekharappa, S., Chitnis, A., Matthews, R. P. and Pack, M. (2004). Inhibition of Jagged-mediated Notch signaling disrupts zebrafish biliary development and generates multi-organ defects compatible with an Alagille syndrome phenocopy. *Development* **131**, 5753-5766.
Lu, S. C., Alvarez, L., Huang, Z. Z., Chen, L., An, W., Corrales, F. J., Avila, M. A., Kanel, G. and Mato, J. M. (2001). Methionine adenosyltransferase 1A knockout mice are predisposed to liver injury and exhibit increased expression of genes involved in proliferation. *Proc. Natl. Acad. Sci. USA* **98**, 5560-5565.
Lu, S. C., Tsukamoto, H. and Mato, J. M. (2002). Role of abnormal methionine metabolism in alcoholic liver injury. *Alcohol* **27**, 155-162.
Luka, Z., Capdevila, A., Mato, J. M. and Wagner, C. (2006). A glycine N-methyltransferase knockout mouse model for humans with deficiency of this enzyme. *Transgenic Res.* **15**, 393-397.
Manco, M., Marcellini, M., Giannone, G. and Nobili, V. (2007). Correlation of serum TNF-alpha levels and histologic liver injury scores in pediatric nonalcoholic fatty liver disease. *Am. J. Clin. Pathol.* **127**, 954-960.
Mari, M., Caballero, F., Colell, A., Morales, A., Caballeria, J., Fernandez, A., Enrich, C., Fernandez-Checa, J. C. and Garcia-Ruiz, C. (2006). Mitochondrial free cholesterol loading sensitizes to TNF- and Fas-mediated steatohepatitis. *Cell Metab.* **4**, 185-198.
Martinez-Chantar, M. L., Vazquez-Chantada, M., Ariz, U., Martinez, N., Varela, M., Luka, Z., Capdevila, A., Rodriguez, J., Aransay, A. M., Matthiesen, R. et al. (2008). Loss of the glycine N-methyltransferase gene leads to steatosis and hepatocellular carcinoma in mice. *Hepatology* **47**, 1191-1199.
Mathurin, P., Deng, Q. G., Keshavarzian, A., Choudhary, S., Holmes, E. W. and Tsukamoto, H. (2000). Exacerbation of alcoholic liver injury by enteral endotoxin in rats. *Hepatology* **32**, 1008-1017.
Mato, J. M., Martinez-Chantar, M. L. and Lu, S. C. (2008). Methionine metabolism and liver disease. *Annu. Rev. Nutr.* **28**, 273-293.
Matthews, R. P., Lorent, K., Russo, P. and Pack, M. (2004). The zebrafish onecut gene hnf-6 functions in an evolutionarily conserved genetic pathway that regulates vertebrate biliary development. *Dev. Biol.* **274**, 245-259.
Matthews, R. P., Plumb-Rudewiez, N., Lorent, K., Gissen, P., Johnson, C. A., Lemaigre, F. and Pack, M. (2005). Zebrafish vps33b, an ortholog of the gene responsible for human arthrogryposis-renal dysfunction-cholestasis syndrome, regulates biliary development downstream of the onecut transcription factor hnf6. *Development* **132**, 5295-5306.
McMaster, C. R. and Bell, R. M. (1997). CDP-choline:1,2-diacylglycerol cholinephosphotransferase. *Biochim. Biophys. Acta* **1348**, 100-110.
Miller, M. W., Duhl, D. M., Winkes, B. M., Arredondo-Vega, F., Saxon, P. J., Wolff, G. L., Epstein, C. J., Hershfield, M. S. and Barsh, G. S. (1994). The mouse lethal nonagouti (a(x)) mutation deletes the S-adenosylhomocysteine hydrolase (Ahcy) gene. *EMBO J.* **13**, 1806-1816.
Pasini, D., Hansen, K. H., Christensen, J., Agger, K., Cloos, P. A. and Helin, K. (2008). Coordinated regulation of transcriptional repression by the RBP2 H3K4 demethylase and Polycomb-Repressive Complex 2. *Genes Dev.* **22**, 1345-1355.
Rawls, J. F., Samuel, B. S. and Gordon, J. I. (2004). Gnotobiotic zebrafish reveal evolutionarily conserved responses to the gut microbiota. *Proc. Natl. Acad. Sci. USA* **101**, 4596-4601.
Sadler, K. C., Amsterdam, A., Soroka, C., Boyer, J. and Hopkins, N. (2005). A genetic screen in zebrafish identifies the mutants vps18, nf2, and foie gras as models of liver disease. *Development* **132**, 3561-3572.
Song, Z., Zhou, Z., Uriarte, S., Wang, L., Kang, Y. J., Chen, T., Barve, S. and McClain, C. J. (2004). S-adenosylhomocysteine sensitizes to TNF-alpha hepatotoxicity in mice and liver cells: a possible etiological factor in alcoholic liver disease. *Hepatology* **40**, 989-997.
Song, Z., Zhou, Z., Song, M., Uriarte, S., Chen, T., Deaciuc, I. and McClain, C. J. (2007). Alcohol-induced S-adenosylhomocysteine accumulation in the liver sensitizes to TNF hepatotoxicity: possible involvement of mitochondrial S-adenosylmethionine transport. *Biochem. Pharmacol.* **74**, 521-531.

Stenkamp, D. L. and Frey, R. A. (2003). Extraretinal and retinal hedgehog signaling sequentially regulate retinal differentiation in zebrafish. *Dev. Biol.* **258**, 349-363.
Streetz, K., Leifeld, L., Grundmann, D., Ramakers, J., Eckert, K., Spengler, U., Brenner, D., Manns, M. and Trautwein, C. (2000). Tumor necrosis factor alpha in the pathogenesis of human and murine fulminant hepatic failure. *Gastroenterology* **119**, 446-460.
Sullivan, K. E., Reddy, A. B., Dietzmann, K., Suriano, A. R., Kocieda, V. P., Stewart, M. and Bhatia, M. (2007). Epigenetic regulation of tumor necrosis factor alpha. *Mol. Cell. Biol.* **27**, 5147-5160.
Tan, J., Yang, X., Zhuang, L., Jiang, X., Chen, W., Lee, P. L., Karuturi, R. K., Tan, P. B., Liu, E. T. and Yu, Q. (2007). Pharmacologic disruption of Polycomb-repressive complex 2-mediated gene repression selectively induces apoptosis in cancer cells. *Genes Dev.* **21**, 1050-1063.
Tanaka, N., Nakanishi, M., Kusakabe, Y., Shiraiwa, K., Yabe, S., Ito, Y., Kitade, Y. and Nakamura, K. T. (2004). Crystal structure of S-adenosyl-L-homocysteine hydrolase from the human malaria parasite Plasmodium falciparum. *J. Mol. Biol.* **343**, 1007-1017.
Thakur, V., McMullen, M. R., Pritchard, M. T. and Nagy, L. E. (2007). Regulation of macrophage activation in alcoholic liver disease. *J. Gastroenterol. Hepatol.* **22 Suppl. 1**, S53-S56.
Tomita, K., Tamiya, G., Ando, S., Ohsumi, K., Chiyo, T., Mizutani, A., Kitamura, N., Toda, K., Kaneko, T., Horie, Y. et al. (2006). Tumour necrosis factor alpha signalling through activation of Kupffer cells plays an essential role in liver fibrosis of non-alcoholic steatohepatitis in mice. *Gut* **55**, 415-424.
Turner, M. A., Yuan, C. S., Borchardt, R. T., Hershfield, M. S., Smith, G. D. and Howell, P. L. (1998). Structure determination of selenomethionyl S-adenosylhomocysteine hydrolase using data at a single wavelength. *Nat. Struct. Biol.* **5**, 369-376.
Villanueva, J. A. and Halsted, C. H. (2004). Hepatic transmethylation reactions in micropigs with alcoholic liver disease. *Hepatology* **39**, 1303-1310.
Wallace, K. N. and Pack, M. (2003). Unique and conserved aspects of gut development in zebrafish. *Dev. Biol.* **255**, 12-29.
Wigg, A. J., Roberts-Thomson, I. C., Dymock, R. B., McCarthy, P. J., Grose, R. H. and Cummins, A. G. (2001). The role of small intestinal bacterial overgrowth, intestinal permeability, endotoxaemia, and tumour necrosis factor alpha in the pathogenesis of non-alcoholic steatohepatitis. *Gut* **48**, 206-211.
Wortham, M., He, L., Gyamfi, M., Copple, B. L. and Wan, Y. J. (2008). The transition from fatty Liver to NASH associates with SAMe depletion in db/db mice fed a methionine choline-deficient diet. *Dig. Dis. Sci.* **53**, 2761-2764.
Xue, G. P. and Snoswell, A. M. (1986). Quantitative evaluation and regulation of S-adenosylmethionine-dependent transmethylation in sheep tissues. *Comp. Biochem. Physiol. B* **85**, 601-608.
Yee, N. S., Lorent, K. and Pack, M. (2005). Exocrine pancreas development in zebrafish. *Dev. Biol.* **284**, 84-101.
Younossi, Z. M., Gorreta, F., Ong, J. P., Schlauch, K., Giacco, L. D., Elariny, H., Van Meter, A., Younoszai, A., Goodman, Z., Baranova, A. et al. (2005). Hepatic gene expression in patients with obesity-related non-alcoholic steatohepatitis. *Liver Int.* **25**, 760-771.
Zhu, X., Song, J., Mar, M. H., Edwards, L. J. and Zeisel, S. H. (2003). Phosphatidylethanolamine N-methyltransferase (PEMT) knockout mice have hepatic steatosis and abnormal hepatic choline metabolite concentrations despite ingesting a recommended dietary intake of choline. *Biochem. J.* **370**, 987-993.

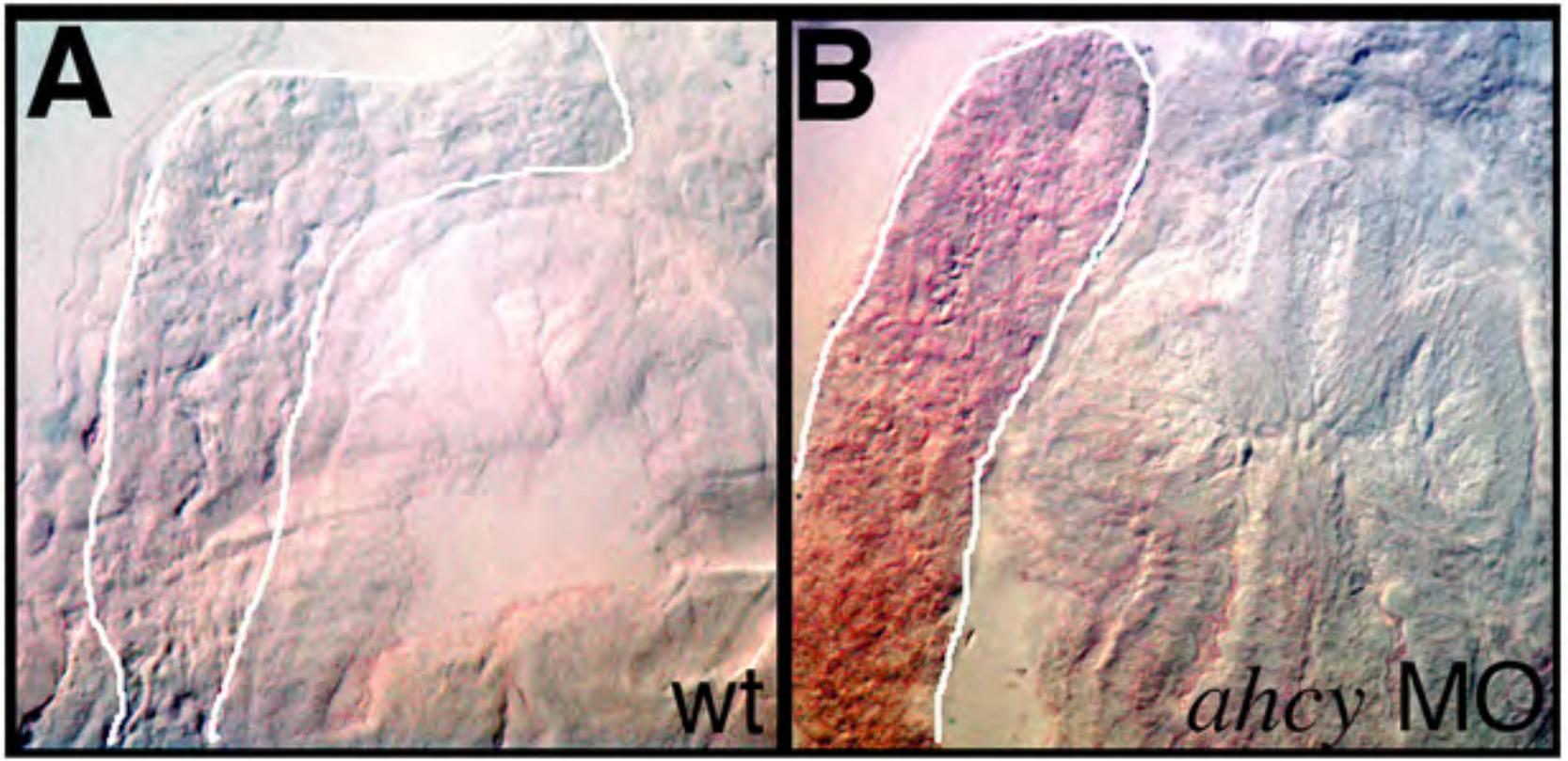
A
wt
B
ahcy MO

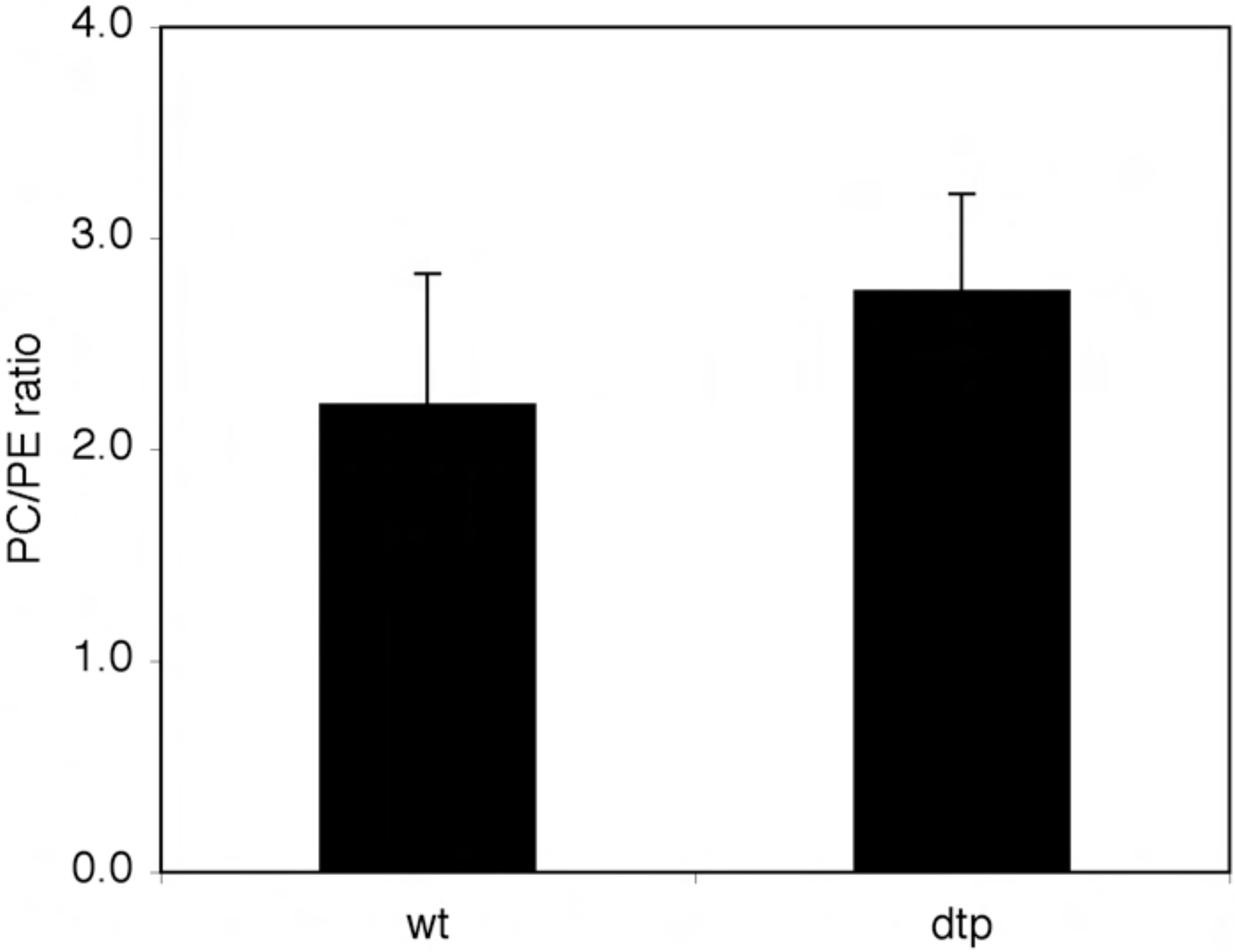
4.0
3.0
2.0
1.0
0.0
PC/PE ratio
wt
dtp

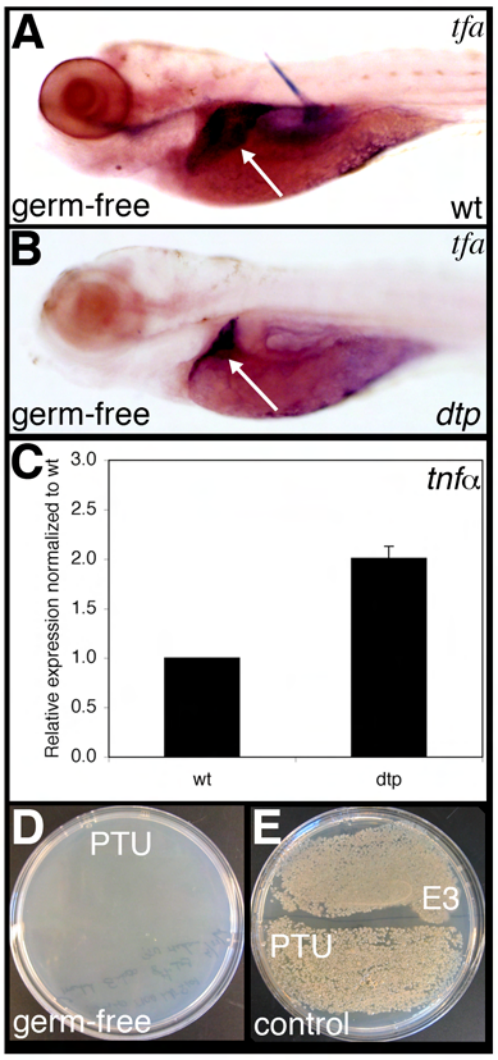
A
tfa
germ-free
wt
B
tfa
germ-free
dtp
C
tnfα
Relative expression normalized to wt
3.0
2.5
2.0
1.5
1.0
0.5
0.0
wt
dtp
D
PTU
germ-free
E
E3
PTU
control

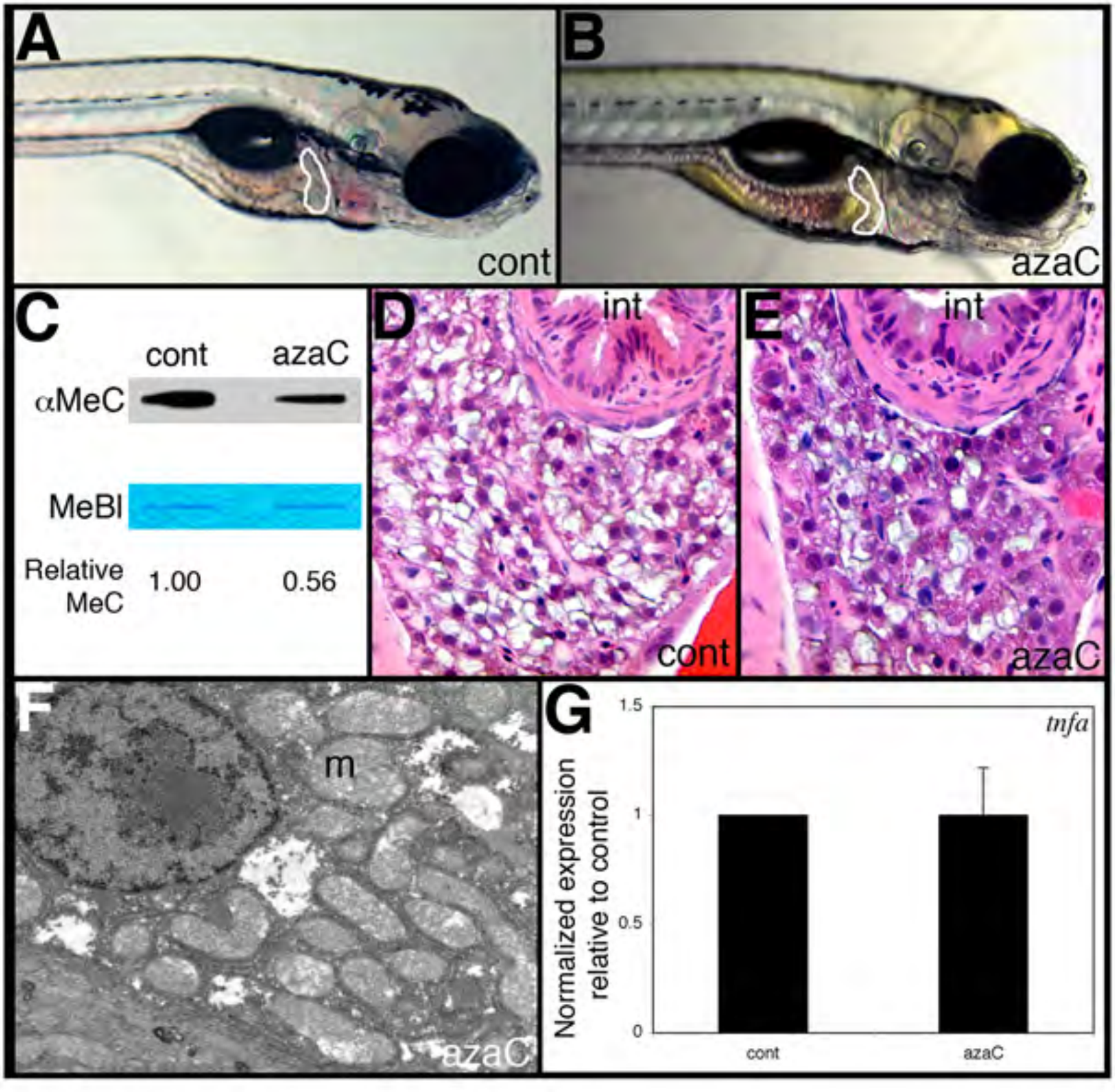
A
cont
B
azaC
C
cont
azaC
αMeC
MeBl
Relative MeC
1.00
0.56
D
int
cont
E
int
azaC
F
m
azaC
G
tnfa
Normalized expression relative to control
1.5
1
0.5
0
cont
azaC

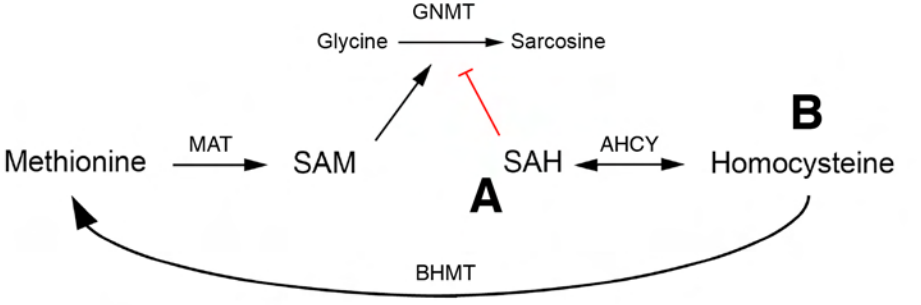
GNMT
Glycine
Sarcosine
Methionine
MAT
SAM
SAH
AHCY
Homocysteine
B
A
BHMT